

**Time Evolution and the Nature of the Near-Infrared Jets in  
GRS1915+105**

S.S. Eikenberry<sup>1</sup> and G.G. Fazio<sup>1</sup>

Harvard-Smithsonian Center for Astrophysics, Cambridge, MA 02138

Received \_\_\_\_\_; accepted \_\_\_\_\_

arXiv:astro-ph/9609181v1 26 Sep 1996

---

<sup>1</sup>Visiting Astronomer, Kitt Peak National Observatory

## ABSTRACT

We observed the galactic microquasar GRS1915+105 in the K ( $2.2\mu\text{m}$ ) band on October 16 and 17, 1995 UTC using the COB infrared (IR) imager on the Kitt Peak National Observatory 2.1-m telescope with a 0.2-arcsec/pixel plate scale and under good ( $\sim 0.7$ -arcsec) seeing conditions. Using a neighboring star in the image frames to determine the point spread function (PSF), we PSF-subtract the images of GRS1915+105. We find no evidence of extended emission such as the apparent near-IR jets seen by Sams *et al.* (1996) in July, 1995. Simple modelling of the star + jet structure allows us to place an upper limit on any similar emission at that position of  $K > 16.4$  at the 95% confidence level, as compared to  $K = 13.9$  as seen by Sams *et al.* (1996). This lack of extended IR flux during continued hard X-ray flaring activity confirms the hypothesis that the extended IR emission arises from the superluminal radio-emitting jets rather than reprocessing of the X-ray emission on other structures around the compact central object. Given the large apparent velocity of the radio-emitting jets, by the time of our observations the Sams *et al.* feature would have moved  $> 1$  arcsec from GRS1915+105, and we can place a limit of  $K > 17.7$  (95% confidence level) on any infrared emission in this region. We can thus place an upper limit on the radiative timescale of the feature of  $\tau < 25$  days, which is consistent with synchrotron jet emission.

*Subject headings:* infrared: stars – stars: individual (GRS 1915+105) –ISM: jets and outflows

## 1. Introduction

The galactic microquasar GRS1915+105 is one of the most intriguing objects in astrophysics today. This object shows hard X-ray, radio, and infrared (IR) flares with variability on timescales from minutes to months (Mirabel and Rodriguez, 1996). In addition, VLA monitoring has revealed collimated ejection events exhibiting superluminal motion interpreted as synchrotron emission from jets with relativistic bulk motions (Mirabel and Rodriguez, 1994). Recently, Sams *et al.* (1996) have reported observations of extended near-IR ( $2.2\mu\text{m}$ ) emission near the beginning of a hard X-ray flare (Sazonov and Sunyaev, 1995). While the position angle of the near-IR extensions is consistent with the radio jets, the nature of the emission is not well-determined. Detailed multi-wavelength studies of the flaring of GRS1915+105 imply the presence of other gas and/or dust in the region surrounding the compact object, in addition to the jets (Mirabel and Rodriguez, 1996). Thus, possible sources of the extended IR flux include reprocessing of the hard X-ray flare on an ejected gas or dust disk, a wind outflow, or the radio jets, or synchrotron emission from the jets themselves (Sams *et al.*, 1996).

## 2. Observations

We observed GRS1915+105 with the COB infrared imager on the Kitt Peak National Observatory<sup>2</sup> 2.1-m telescope on October 16 and 17, 1995, roughly 3 months after Sams *et al.* (1996). We used the K-band ( $2.2\mu\text{m}$ ) filter, with a 0.2-arcsec/pixel plate scale. On October 16, we took four 30-second exposures through light cirrus, with seeing of  $\sim 0.7$ -arcsec full-width half-maximum (FWHM). On October 17, we again took four 30-second exposures, this time under photometric conditions, but with  $\sim 1.1$ -arcsec FWHM

---

<sup>2</sup>KPNO is operated by AURA Inc. under contract to the National Science Foundation.

seeing. During each sequence of exposures, we moved the telescope around the position of GRS1915+105 in order to avoid defects in the array. We subtracted the sky background and flatfielded each exposure, and then combined each set of four exposures. Figure 1 shows a contour map of the resulting image for the October 16 data. Photometry of the combined images gives K-band magnitudes of  $K = 13.51 \pm 0.05$  on October 16 and  $K = 13.43 \pm 0.03$  on October 17 (see also Eikenberry and Fazio, 1995).

### 3. Analysis

#### 3.1. Limits on point-like emission

In our analysis, we first concentrate on possible emission from a feature similar to that seen by Sams *et al.* (1996). While the separation between the stellar counterpart of GRS1915+105 and the extension of Sams *et al.* (1996) is less than 1/2 of our image FWHM, if the feature’s brightness ( $K = 13.9$ ) remained constant it would be the source of 60% of the photons in our images, and simple PSF-subtraction should reveal its presence. From each of the background-subtracted and flatfielded (but uncombined) 30-second exposures, we extract a  $5 \times 5$ -arcsec region centered on GRS1915+105. For our PSF, we extract an identical region centered on a star near GRS1915+105 with a very similar K-band flux (Star A in Figure 1). For each exposure, we scale the PSF and subtract it from the images of GRS1915+105. We see no evidence for extended structure in any of the PSF-subtracted exposures. We then combine the four PSF-subtracted exposures for each night. Again, we find no evidence for extended structure in the combined PSF-subtracted images (see Figure 2).

We then apply a simple sliding-cell source-detection algorithm to the PSF-subtracted images. In this approach, we take a model PSF (a 2-D gaussian fit to Star A) and center it

on a pixel in the image. We multiply the image pixel values by the corresponding PSF values at their location, and sum to obtain the total of the products. We then perform the same operation on the error image for the PSF-subtracted image (including the uncertainties in the PSF), summing the error products in quadrature. The ratio of the image sum to the error sum then gives the statistical significance of any point source at the image pixel location. Applying this algorithm to the PSF-subtracted images from both nights, we find no source with a statistical significance  $> 1\sigma$  at any location.

In order to estimate the sensitivity of our observations and analysis techniques, we perform a simple Monte Carlo simulation. First, we model the GRS1915+105 region as 2 point sources separated by 0.3-arcsec - the star plus a southern jet - as seen by Sams *et al.* (1996). We ignore the northern jet due to its much lower flux. Second, (using the model PSF for both point sources), we select a relative normalization of the model PSFs for the two point sources, scale and add them with the appropriate positional offsets, and then rescale the sum to give the same number of counts as in the real GRS1915+105 image. Next, we add normally-distributed random numbers (having standard deviations determined from the quadrature-summed uncertainties of both the GRS1915+105 and Star A (PSF) images) to each pixel of the simulated image. Finally, we take the image of Star A, scale it, and subtract it from the simulated image, exactly as with the actual GRS1915+105 images.

In Figure 3, we present a typical simulated result of the PSF subtraction for an extended component with  $K = 13.9$ . If the extended emission seen by Sams *et al.* (1996) had remained unchanged, we would have unambiguously found it in our data on both nights. In order to place an upper limit on any point-like flux at this position, we then decrease the flux of the extended emission in the model and repeat the simulation process. We set our upper limit on the flux of the extended component at the point where, for 100

Monte Carlo simulations as described above, we detect the extended component in the PSF-subtracted image at the 95% confidence level using the sliding-cell source-detection algorithm. For October 16, the limit is  $K > 16.4$ , while for October 17 (when the seeing was poorer), the limit is  $K > 15.8$ .

### 3.2. Limits on extended emission

The limit on point-like emission is useful in confirming that the Sams *et al.* (1996) feature was transient, as expected for emission from the radio-emitting jets. However, since this feature is associated with the radio-emitting jets of GRS1915+105, it will exhibit superluminal motion, and may also expand at high velocities. Thus, we have performed further analyses searching for possible non-point-like emission from the jet.

We perform this search using, once again, the sliding-cell algorithm described above. However, instead of using Star A as a PSF, we use a broadened PSF for the jet emissions. Applying the algorithm to the stellar-PSF-subtracted images, we find no evidence of extended emission using trial jet-PSFs with FWHM values of 0.8, 1.0, 1.25, and 1.5 arcsec. Given that the Sams *et al.* feature was point-like with their  $\sim 0.2$  arcsec resolution, even if the feature expanded at  $0.5c$  (much faster than the limit for the radio-emitting jets), it could have expanded only to a FWHM of 1.25 arcsec, given the 12.5 kpc distance to GRS1915+105 (Rodriguez *et al.*, 1995). Thus, we conclude that there is no evidence for infrared jet emissions in our data.

As with the point-like emission, we perform a Monte Carlo simulation to estimate the sensitivity of our observations and analysis techniques. We now assume that the jet has moved 1.2 arcsec farther from GRS1915+105 - an apparent velocity of  $1.0c$ , which is less than is observed in the radio jets (Mirabel and Rodriguez, 1994). We also assume

a worst-case jet FWHM of 1.5 arcsec for the source-detection algorithm - an expansion velocity  $> 0.5c$ , which is much greater than observed in the radio jets. This approach gives an upper limit of  $K > 17.7$  at the 95% confidence level for any infrared jet emission.

#### 4. Discussion

Given that the hard X-ray flaring activity which began in late June or early July 1995 (Sazonov and Sunyaev, 1995) continued through the time of these observations (Harmon *et al.*, 1995), the drop of a factor  $> 10$  in the  $2.2\mu\text{m}$  flux at the observed location of Sams *et al.* (1996) places strong constraints on several of the proposed explanations for the extended near-IR emission. In particular, hypotheses involving the reprocessing of the X-ray emission on stellar winds, ejected dust or gas disks, or other steady-state or slow-moving structures do not appear to explain such behavior. This, in addition to the appearance of the IR features oppositely oriented about GRS1915+105, their position angle match with the radio jets, and the similarities of the North/South flux asymmetry to that in the radio (Sams *et al.*, 1996), seems to confirm the identification of the features seen by Sams *et al.* as infrared jets.

If the features are indeed due to infrared jets, then by the time of our observations, the southern (bright) jet would have moved more than 1 arcsec from GRS1915+105, and we have an upper limit of  $K > 17.7$  in this region. If the near-IR flux arises from reprocessing of the X-ray emission on the jet, the reprocessing efficiency may have dropped by this factor  $> 33$  due to the increased distance between the X-ray source and the jet and/or changes in the X-ray opacity of the jets. Alternatively, if the IR flux arises from synchrotron processes in the jet, then we can place an upper limit on the radiative lifetime of the IR-emitting particles, using the time separation between our observations and those of Sams *et al.* (1996) and the fact that our upper limit is a factor 33 lower in flux than

the Sams *et al.* feature. Thus, we find that the  $1/e$  radiative lifetime of the IR-emitting electrons is  $\tau < 26$  days. For synchrotron emission, the relativistic electrons producing the IR emission have shorter radiative lifetimes than the radio-emitting electrons by a factor of  $\sqrt{\nu_{IR}/\nu_{radio}} \sim 10^2$ , independent of the magnetic field strength. Since the radio-emitting jets have lifetimes significantly less than 1 year, we find that our limits are compatible with the hypothesis that the Sams *et al.* feature arises from synchrotron processes in the radio-emitting jets.

## 5. Conclusions

We have presented near-infrared K ( $2.2\mu\text{m}$ ) band observations of the galactic microquasar GRS1915+105 on October 16 and 17, 1995 with a 0.2 arcsec/pixel plate scale under good seeing conditions. Using PSF subtraction of the stellar image of GRS1915+105, we find no evidence of near-infrared emissions as seen by Sams *et al.* (1996) in July, 1995. Simple modelling shows that we would have detected any such extended emission at the 95% confidence level down to a limit of  $K > 16.4$ , as compared to the  $K = 13.9$  jet observed by Sams *et al.* (1996). The fact that the IR flux at this location dropped by a factor  $> 10$  during a time when the hard X-ray flux increased seems to rule out reprocessing of the hard X-ray emission on slow-moving or steady-state structures near the compact object as a viable explanation for the extended IR emission, and confirms the hypothesis that the extended IR emission arises from the radio-emitting jets.

If the features are indeed due to infrared jets, then by the time of our observations, the southern (bright) jet would have moved more than 1 arcsec from GRS1915+105, and we have an upper limit of  $K > 17.7$  in this region, a factor of  $> 33$  drop in the IR flux. This allows us to place an upper limit on the radiative lifetime of the feature of  $\tau < 26$  days. These limits are consistent with the hypothesis that the Sams *et al.* feature was due to



synchrotron processes in the radio-emitting jets of GRS1915+105.

We would like to thank I.F. Mirabel for bringing the near-IR jets in GRS1915+105 to our attention, M. Merrill for assisting with the COB observations, and the anonymous referee for his/her helpful comments. S. Eikenberry is supported by a NASA Graduate Student Researchers Program fellowship through Ames Research Center.

## REFERENCES

- Eikenberry, S.S. and Fazio, G.G., 1995, IAU Circular 6267.
- Harmon, B.A., Paciesas, W.S., Zhang, S.N., Deal, K.J., 1995, IAU Circular 6266.
- Mirabel, I.F. and Rodriguez, L.F., 1996, in *Proceedings of the NATO ASI on Solar and Astrophysical Magnetohydrodynamic Flows*, in press.
- Mirabel, I.F. and Rodriguez, L.F., 1994, *Nature*, **335**, 46.
- Rodriguez, L.F., Gerard, E., Mirabel, I.F., Gomez, Y., Velazquez, A. 1995, *ApJS*, 101, 173.
- Sams, B.J., Eckart, A., Sunyaev, R., 1996, *Nature*, 382, 47.
- Sazonov, S. and Sunyaev, R., 1995, IAU Circular 6196.

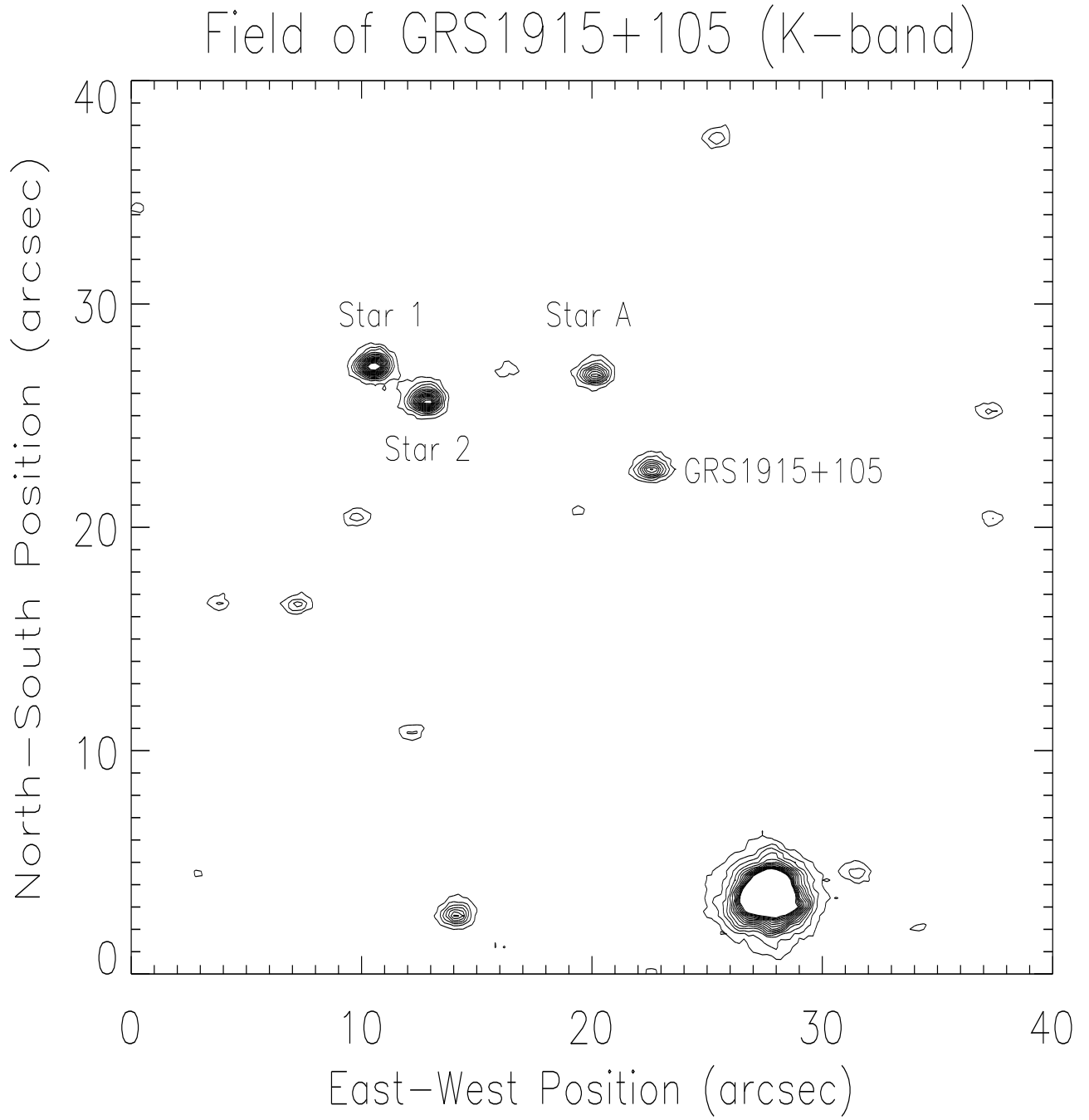


Fig. 1.— K-band ( $2.2\mu\text{m}$ ) map of the 40-arcsec field surrounding GRS1915+105

# PSF-Subtracted Image of GRS1915+105

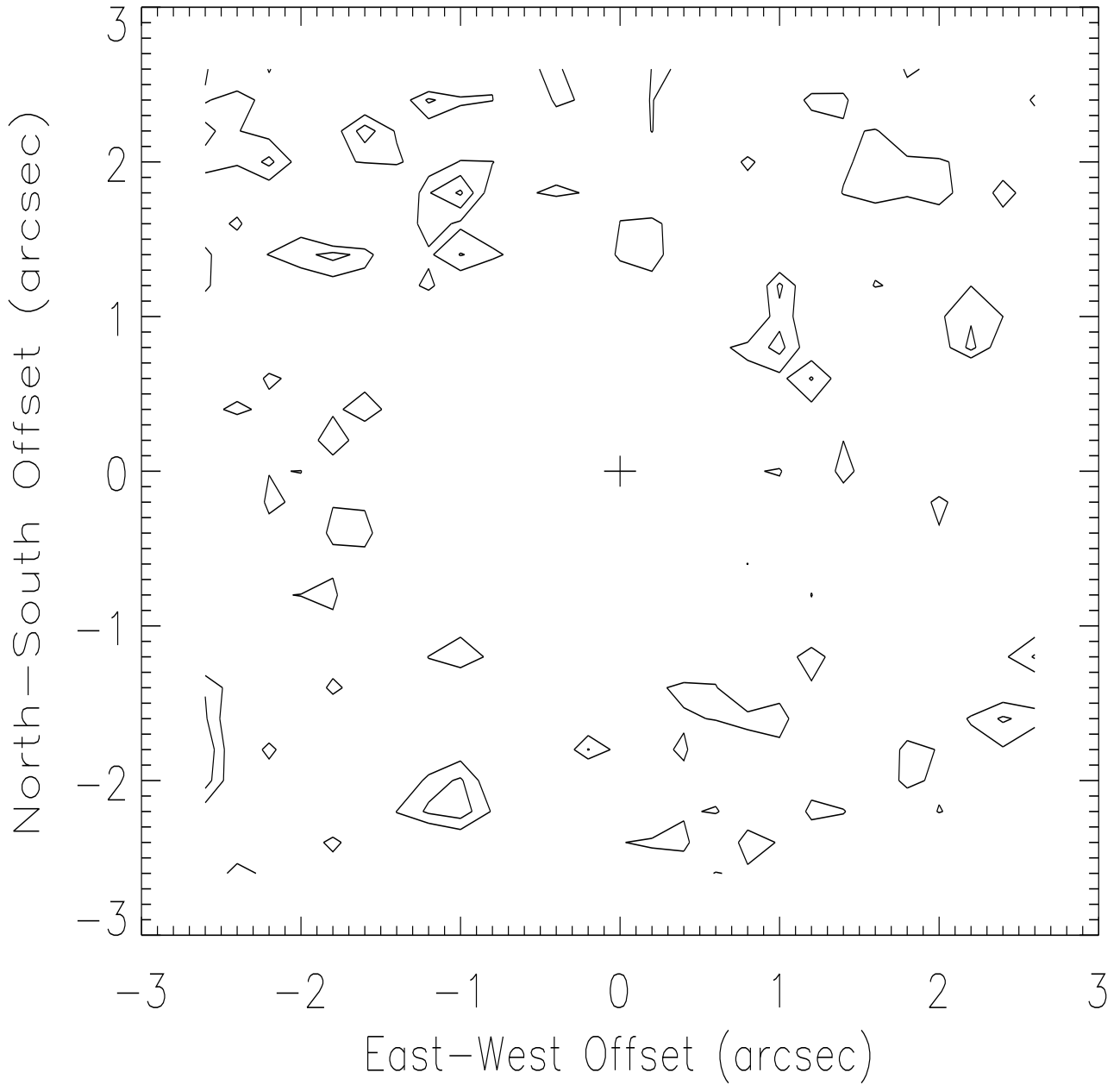


Fig. 2.— PSF-subtracted map of the 5-arcsec square region centered on GRS1915+105. Contours are drawn at levels of  $1\sigma, 2\sigma, 3\sigma, \dots$ . No significant residuals are evident.

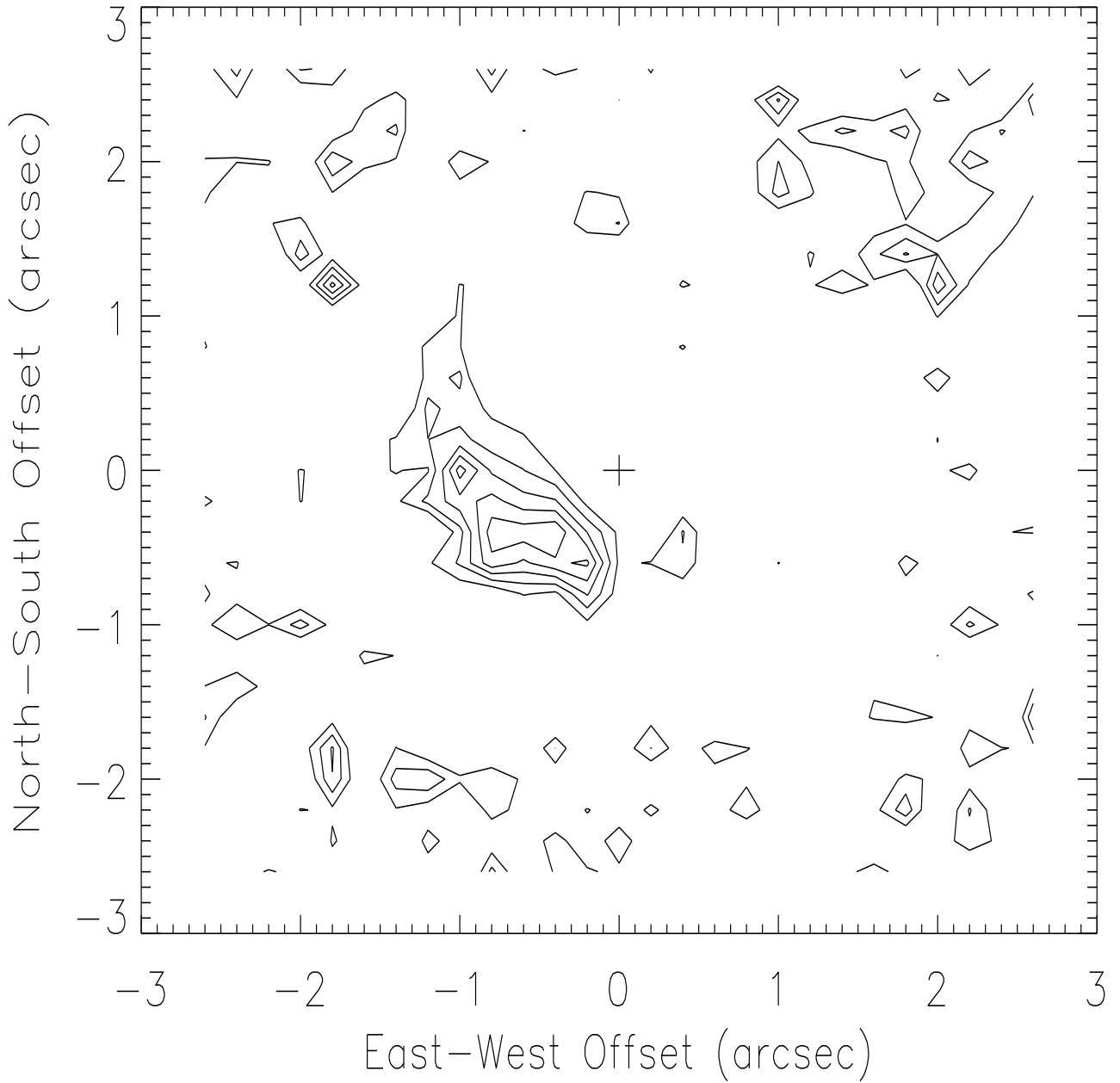


Fig. 3.— PSF-subtracted map of the 5-arcsec square region centered on a simulated image of GRS1915+105 including a jet component with  $K=13.9$  at a 0.3-arcsec separation. Contours are the same as in Figure 2. The presence of such a jet component would be clearly evident if it were present in the actual data (Figure 2).